

Autonomous Ratcheting by Stochastic Resetting

Pulak K. Ghosh^{1*}, Shubhadip Nayak¹, Jianli Liu², Yunyun Li², and Fabio Marchesoni^{2,3†}

¹ Department of Chemistry, Presidency University, Kolkata 700073, India

² Center for Phononics and Thermal Energy Science,

Shanghai Key Laboratory of Special Artificial Microstructure Materials and Technology,
School of Physics Science and Engineering, Tongji University, Shanghai 200092, China and

³ Dipartimento di Fisica, Università di Camerino, I-62032 Camerino, Italy

(Dated: July 13, 2023)

We propose a generalization of the stochastic resetting mechanism for a Brownian particle diffusing in a one-dimensional periodic potential: randomly in time, the particle gets reset at the bottom of the potential well it was in. Numerical simulations show that in mirror asymmetric potentials, stochastic resetting rectifies the particle's dynamics, with maximum drift speed for an optimal average resetting time. Accordingly, an unbiased Brownian tracer diffusing on an asymmetric substrate can rectify its motion by adopting an adaptive stop-and-go strategy. Our proposed ratchet mechanism can model directed autonomous motion of molecular motors and micro-organisms

PACS numbers:

The notion of stochastic resetting (SR) is attracting growing attention (see Ref.¹ for a recent review). This term refers to the sudden interruption of a stochastic process after random time intervals, followed by its starting anew, possibly after a further latency time, with same initial conditions. Diffusion under SR is a non-equilibrium stationary process, which found applications in search contexts², optimization of randomized computer algorithms³, and in many biophysical problems^{4,5}. Surprisingly, under SR the otherwise infinite mean first passage time of a freely diffusing Brownian particle⁶ from an injection point to an assigned target point becomes finite, and, most notably, can be minimized for an optimal choice of the resetting time, τ ^{8,9}. Many analytical methods earlier developed in the theory of homogeneous stochastic processes^{6,7} can be generalized to study diffusion under SR, for instance, to calculate the mean-first-exit time (MFET) of a reset particle out of a one-dimensional (1D) domain¹⁰ or potential well¹¹. In general, SR speeds up (slows down) diffusive processes characterized by random escape times with standard deviation larger (smaller) than the respective averages⁵.

In this Letter we propose an SR mechanism with degenerate resetting point. Let us consider an overdamped Brownian particle of coordinate x , diffusing in a 1D periodic potential, $V(x)$, of period L . We assume for simplicity that the potential unit cells have one minimum each at $x_n = x_0 + nL$, with $n = 0, \pm 1, \dots$. Upon resetting, the particle stops diffusing and falls instantaneously at the bottom of the potential well it was in; it will resume diffusing after a latency time $\tau_0 \geq 0$, see Fig. 1(a). By this mechanism of *autonomous* SR, we intend to model the dynamics of small motile tracers (like bacteria or micro-robots¹²) capable of switching their internal engine on and off. In the case of undirected motility, the tracer

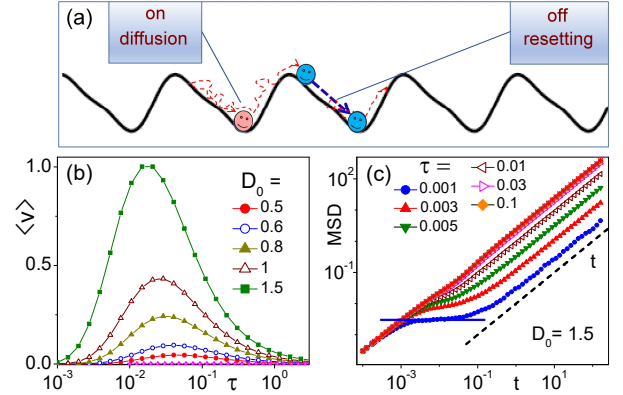


FIG. 1: Autonomous ratcheting by stochastic resetting: (a) schematics; (b) $\langle v \rangle$ vs τ for different D_0 ; (c) MSD vs t for $D_0 = 1.5$ and different τ . The asymptotic dependence is linear in t (dashed line), while the horizontal plateaus for very low τ come close to the square half-width of the relevant probability density peak, $\langle (x - x_0)^2 \rangle \simeq 2D_0\tau$, given in the text (see, e.g., the solid line for $\tau = 10^{-3}$). Values of the diffusion constant, D , obtained by fitting Eq. (3) are plotted in Fig. 2(c). Numerical simulations for the ratchet potential of Eq. (2) with $L = 1$ and $\tau_0 = 0$.

would perform an unbiased Brownian motion. Let us further assume that the barriers separating two adjacent potential minima are asymmetric under mirror reflection, i.e., $V(x - x_0) \neq V(-x + x_0)$ (ratchet potential¹³). Extensive numerical simulations show that (i) SR *rectifies diffusion* in a ratchet potential. The particle's net drift speed, $\langle v \rangle$, reaches a maximum for an optimal value of the resetting time, τ , which strongly depends on the potential profile, see Fig. 1(b); (ii) SR suppresses spatial diffusion. For large observation times, the particle's mean-square displacement (MSD) turns proportional to time (normal diffusion); the relevant diffusion constant increases sharply with the resetting time in correspondence with the maximum of the drift speed, see Fig. 1(c).

*pulak.chem@presiuniv.ac.in (corresponding author)

†fabio.marchesoni@pg.infn.it (corresponding author)

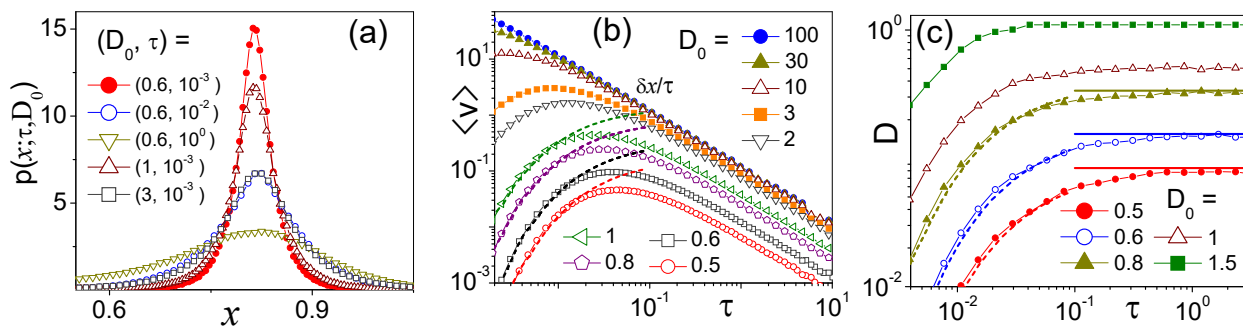


FIG. 2: Simulation data analysis: (a) $p(x; \tau, D_0)$ for different values of D_0 and τ ; (b) $\langle v \rangle$ vs. τ for different D_0 . The dashed curves are our predictions respectively for small τ , $\langle v \rangle = L/\langle T(\tau) \rangle$, and in the strong noise regime, $\langle v \rangle = \delta x/\tau$ with $\delta x = (L_L - L_R)/2$; (c) fitting parameter, D , of the diffusion law of Eq. (3), also for different D_0 . Our analytical estimates for small and large τ (see text) are represented respectively by dashed and solid curves. Numerical simulations for the ratchet potential of Eq. (2) with $L = 1$ and $\tau_0 = 0$.

While this variant of the SR mechanism may be reminiscent of a flashing ratchet with pulsated temperature¹⁴, here the diffusing tracer exploits the substrate spatial asymmetry to autonomously rectify its random motion in the absence of external time-dependent fields of force or gradients^{13,18,19}, simply by time-operating its internal engine to adjust to the substrate itself.

Model. The simulated particle dynamics was formulated in terms of the Langevin equation (LE),

$$\dot{x} = -V'(x) + \xi(t), \quad (1)$$

where $\xi(t)$ denotes a stationary zero-mean valued Gaussian noise with autocorrelation $\langle \xi(t)\xi(0) \rangle = 2D_0\delta(t)$ (white noise) and $V(x)$ is the standard ratchet potential¹³,

$$V(x) = \sin(2\pi x/L) + (1/4)\sin(4\pi x/L), \quad (2)$$

with asymmetric barriers of height $\Delta V = (3/2)(1 + 2/\sqrt{3})^{1/2} \simeq 2.20$. The potential unit cell $[0, L]$ has a maximum (barrier) at $x_b = (L/2\pi) \arccos[(\sqrt{3}-1)/2] \simeq 0.19L$ and a minimum (well bottom) at $x_0 = L - x_b \simeq 0.81L$, with curvatures $\omega_0^2 = V''(x_0) = -V''(x_b) = (2\pi/L)^2(3\sqrt{3}/2)^{1/2} \simeq 63.6/L^2$, see Fig. 1(a). The asymmetric potential wells have right/left slopes of different lengths, $L_{R,L}$, with $L_L = x_0 - x_b = L - L_R \simeq 0.62L$. In addition to the thermal fluctuations and the ratchet potential, the particle is subjected to resetting to the attracting local substrate minimum after a random time that is taken from exponential distribution with mean $\tau = 1/r$. Where, r is the resetting rate. Partly motivated by technical issues in experiments, earlier works²⁰⁻²² had considered the case when the particle was reset to a fully randomly chosen position. Along with the restart protocol, the Eq.(1) was numerically integrated by means of a standard Milstein scheme¹⁵, to compute the drift speed $\langle v \rangle = \lim_{t \rightarrow \infty} [x(t) - x(0)]/t$, and the asymptotic MSD,

$$\langle \Delta x^2(t) \rangle = \langle x^2(t) \rangle - \langle v \rangle^2 t^2 \equiv 2Dt, \quad (3)$$

of a particle under stationary conditions (with or without SR), (Figs. 1 and 2), and the MFET's, $\langle T_{R,L}(\tau) \rangle$, for a reset particle injected at the bottom of the well, x_0 , to first exit it through the left (right) barrier, x_b ($x_b + L$) (Fig. 3).

Rectification under SR. The key features of the resulting SR ratchet are illustrated in the bottom panels of Fig. 1: the particle motion gets rectified with net speed $\langle v(\tau) \rangle$ [Fig. 1(b)] and asymptotic diffusion constant, $D(\tau)$, a monotonically increasing function of the SR time [Fig. 1(c)]. Rectification is maximum in an optimal τ range, as D approaches an stationary value (the same as in the absence of SR).

To explain ratcheting under SR we anticipate two properties of the statistics of particle escape out of a potential well, summarized in Fig. 3. In the absence of resetting, i.e., for asymptotically large τ , the probability current density of the process is zero, which rules out rectification¹³, $\langle v(\infty) \rangle = 0$. Things change upon decreasing the SR time, as proven by the τ -dependence of the splitting probabilities, $\pi_{R,L}(\tau)$, for the particle to exit a potential well through the right/left barrier. Upon lowering τ , the asymmetry ratio π_R/π_L in Fig. 3(b) grows monotonically, the effect being more apparent at low noise, $D_0 \ll \Delta V$, so that $\langle v(\tau) \rangle > 0$. We qualitatively explain this property with the increased asymmetry of the probability density⁶ of the reset particle around the potential minima [Fig. 2(a)]. On the other hand, the data of Fig. 3(b) clearly show that in the limit $\tau \rightarrow 0$, $\langle T_R(\tau) \rangle$ diverges exponentially, so that we anticipate $\langle v(\tau \rightarrow 0) \rangle = 0+$. The combination of these two opposite effects determines the typical resonant profile of the $\langle v(\tau) \rangle$ curves.

Slow SR. More in detail, the data of Fig. 2(b) suggest that $\langle v(\tau) \rangle$ decays asymptotically like τ^{-1} . This behavior can be easily explained in the strong noise regime with $D_0 \gg \Delta V$ and $\langle T_{R,L}(\tau) \rangle \ll \tau$. Under this condition, the particle executes many barrier crossings before being reset at the bottom of a $V(x)$ well. At resetting, it is

caught in average to the left of the well bottom; hence, at each resetting the particle jumps to the right an average distance, $\delta x = \bar{x} - x_0 > 0$, \bar{x} being the center of mass of the (periodic) particle's stationary probability density function, $p(x; \tau, D_0)$, in the potential well with bottom at $x = x_0$. Accordingly, the particle gets rectified with positive net drift speed $\langle v(\tau) \rangle = \delta x / \tau$. In the strong noise regime, $p(x; \tau, D_0)$, approaches a uniform distribution; hence, $\delta x = (L_L - L_R)/2$, in good agreement with the numerical data of Fig. 2(a).

Upon decreasing the noise strength, δx diminishes for two reasons, as illustrated in Fig. 2(a). Firstly, in the absence of SR, i.e., for $\tau \rightarrow \infty$, the probability density, $p(x; \tau, D_0)$, approaches its thermal equilibrium form, $p(x; \infty, D_0) = \mathcal{N} \exp(-V(x)/D_0)$, with \mathcal{N} an appropriate normalization constant. For $D_0 \ll \Delta V$, $p(x; \infty, D_0)$ shrinks around x_0 , that is, δx diminishes. Secondly, by lowering D_0 in the presence of SR, i.e., for finite τ , $\langle T(\tau) \rangle$ grows comparable with τ . Accordingly, barrier escape and resetting events grow correlated, which invalidates the above estimate of the particle's drift speed. However, numerical data confirm that $\langle v(\tau) \rangle$, though strongly suppressed, keeps decaying asymptotically like $1/\tau$, even at low noise.

Fast SR. The plots of $p(x; \tau, D_0)$ for the lowest τ values in Fig. 2(a) consist of a central peak tapering off with asymmetric slow-decaying tails on both sides. In the limit $\tau \rightarrow 0$, (i) the peak gets sharper and more symmetric, while remaining centered at the resetting point, x_0 . Its square half-width can be easily calculated for $D_0 \ll \Delta V$, by approximating $V(x) \simeq \omega_0^2(x - x_0)^2/2$ and averaging over the SR time, that is, $\langle (x - x_0)^2 \rangle \simeq 2D_0\tau/(1 + 2\omega_0^2\tau)$; (ii) the tails get thinner but more asymmetric. This behavior is consistent with the τ -dependence of the escape asymmetry ratio, π_R/π_L , displayed in Fig. 3(b)⁶.

The sharp decay of $\langle v(\tau) \rangle$ for $\tau \rightarrow 0$ proves that fast SR eventually suppresses the interwell particle diffusion. In such limit, as shown in Fig. 3, the particle tends to jump to the right, with $\pi_R(\tau) \gg \pi_L(\tau)$ and, therefore, $\langle T(\tau) \rangle \simeq \langle T_R(\tau) \rangle$ with $\langle T(\tau) \rangle \gg \tau$. Under these conditions, the resulting drift speed can be easily estimated under renewal theory approximation¹⁶, that is $\langle v(\tau) \rangle = L/\langle T_R(\tau) \rangle$.

To calculate $\langle T_R(\tau) \rangle$ we had recourse to the analytical results of Ref.¹¹ for Brownian diffusion under SR in the presence of a constant bias. We made contact with Eq. (6) there, by replacing the constant bias with the effective (right-to-left) restoring force of our ratchet potential, $\Delta V/L_R$. In the limit $\tau \rightarrow 0$, the MFET for the transition to the adjacent well on the right, $x_0 \rightarrow x_0 + L$, is twice the MFET for the transition $x_0 \rightarrow x_b + L$, that is

$$\langle T(\tau) \rangle \simeq \langle T_R(\tau) \rangle \simeq 2\tau \exp\left(\Delta V/2D_0 + L_R/\sqrt{D_0\tau}\right). \quad (4)$$

Of course, this approximation holds good only for $\pi_R(\tau) \simeq 1$ ($\pi_L(\tau) \simeq 0$), and its agreement with

the numerical data improves upon decreasing the noise strength, i.e., for $D_0 \lesssim \Delta V$, as shown in Fig. 3(a). On making use of this estimate for $\langle T_R(\tau) \rangle$, we closely reproduced also the raising branches of the $\langle v(\tau) \rangle$ curves in Fig. 2(b).

Diffusion under SR. Regarding the intrawell diffusion, we remind that in the absence of SR, the MFET from x_0 to $x_0 \pm L$ amounts to the standard Kramers' time⁷ $T_K = (2\pi/\omega_0^2) \exp(-\Delta V/D_0)$. By the same token, one concludes that for $\tau \rightarrow \infty$, $\langle T_R \rangle \simeq \langle T_L \rangle$, with both MFET's tending to T_K for $D_0/\Delta V \rightarrow 0$, and their ratio, $\langle T_R \rangle/\langle T_L \rangle$ approaching $(1 + L/L_L)/(1 + L/L_R) \simeq 0.72$ in the opposite limit, $D_0/\Delta V \rightarrow \infty$. On the other hand, for large τ the splitting probabilities can be easily computed assuming no SR (see Sec. 5.2.7 of Ref.⁷); their limits for $D_0/\Delta V \rightarrow 0$ (and $\rightarrow \infty$) are respectively $\pi_{R,L}(\infty) = 1/2$ (and $L_{L,R}/L$), as shown in Fig. 3(b).

These remarks are useful to interpret the MSD data sets of Fig. 1(c). Numerical simulation indicates that diffusion at large times, $t \gg \langle T(\tau) \rangle$, is normal, as anticipated by the fitting law of Eq. (3). At small τ , a transient plateau for $t \lesssim \langle T(\tau) \rangle$, $\langle \Delta x^2 \rangle \simeq 2D_0\tau$, marks the particle relaxation inside a single potential well [with $\langle \Delta x^2 \rangle$ of the order of the square half-width of the $p(x; \tau, D_0)$ peak estimated above]. The τ -dependence of the asymptotic diffusion constants, D , is reported in Fig. 2(c). For large τ , the $D(\tau)$ curves approach the horizontal asymptotes⁷, $D = L^2/2T_K$, as to be expected in the absence of SR. Vice versa for very short SR times, the diffusion constant is well approximated by $D(\tau) = L^2/2\langle T_R(\tau) \rangle$, as predicted by the renewal theory for a process with average escape time constant $\langle T_R(\tau) \rangle$ ¹⁶. In both τ limits, our phenomenological arguments are supported by numerical simulation.

Comparison with standard diffusion under SR. Numerical data in Fig. 3(a) show that by decreasing the SR time, $\langle T_R(\tau) \rangle$ keeps being larger than $\langle T_L(\tau) \rangle$. Moreover, $\langle T(\tau) \rangle$ grows monotonically with τ , i.e., the MFET out of the potential well is not optimized by resetting. Of course, the predicted SR optimization of the average passage times⁸ is still detectable, but only for the unconstrained transitions $x_0 \rightarrow x_b$ with $x \geq x_b$, and $x_0 \rightarrow x_b + L$ with $x \leq x_b + L$. In panel (c) of Fig. 3 we investigated the same transitions as in panel (a), except for the reflecting barriers, which were shifted at $\mp\infty$. The corresponding right/left unconstrained MFPT curves, $\langle T_{R,L}^{(u)}(\tau) \rangle$, overlap throughout the entire τ range. Furthermore, all MFPT curves diverge for $\tau \rightarrow \infty$, as to be expected due to the lack of a reflecting barrier⁸. In the absence of SR (i.e., for $\tau \rightarrow \infty$), the particle still diffuses over the substrate like a free particle, but with the reduced effective diffusion constant, $D = L^2/2T_K$, of Eq. (3) [see fits in Fig. 2(c)]. This suggests rewriting Eq. (7) of Ref.⁸ as

$$\langle T_{R,L}^{(u)}(\tau) \rangle / \tau = \exp(L/\sqrt{D\tau}) - 1, \quad (5)$$

a formula that well reproduces the large- τ branches of the curves in Fig 3(c) with no additional fitting parameters.

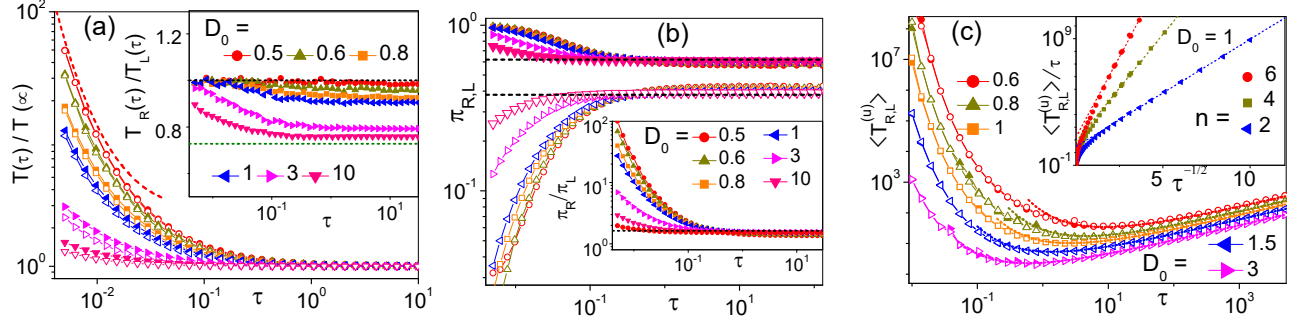


FIG. 3: Exit time statistics: (a) MFET's out of a potential well through the right/left barrier, $\langle T_{R,L} \rangle$, or through either barrier, $\langle T \rangle$; (b) splitting probabilities, $\pi_{R,L}$, for right/left exits (solid/empty symbols), vs τ for different D_0 (see legends). Note that $\langle T \rangle = \pi_R \langle T_R \rangle + \pi_L \langle T_L \rangle$ ⁶. The dashed curve in (a) represents the analytical estimate of $\langle T(\tau) \rangle \simeq \langle T_R(\tau) \rangle$ for $\tau \rightarrow 0$, Eq. (4), with $\langle T(\infty) \rangle = T_K$ (see text). The dashed lines in (b) are the large D_0 limits of $\pi_{R,L}(\infty) = L_{L,R}$ (with the corresponding ratio displayed in the inset). The horizontal lines in the inset of (a) are the expected $\langle T_R \rangle / \langle T_L \rangle$ ratios for $D_0 \rightarrow 0$ (upper) and ∞ (lower, see text). (c) unconstrained right/left MFPT's, $\langle T_{R,L}^{(u)} \rangle$, $x_0 \rightarrow x_0 \pm L$, (empty/solid symbols) for different values of D_0 ; inset: small- τ dependence of the MFPT's for multiple cell transitions, $x_0 \rightarrow x_0 + nL$, for $D_0 = 1$. Simulation data are compared with the relevant estimates of Eqs. (5) (large τ) and (6) (small τ). Numerical simulations for the ratchet potential of Eq. (2) with $L = 1$ and $\tau_0 = 0$.

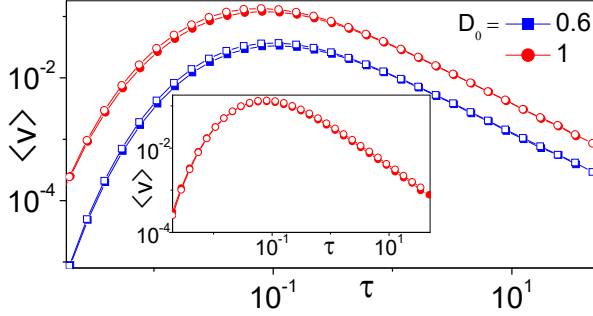


FIG. 4: Rectification speed, $\langle v(\tau) \rangle$, of the SR ratchet of Fig. 1 with $\tau_0 = 0.1$ (filled symbols) and $\tau_0 = 0$ (empty symbols), for different D_0 . The zero-latency data have been rescaled according to Eq. (7). Inset: $\langle v(\tau) \rangle$ of a flashing ratchet with dichotomic noise strength, $D_0(t)$, switching between 0 (fixed waiting time $\tau_0 = 0.1$) and D_0 (random waiting times exponentially distributed with average τ), compared with the flashing ratchet in the main panel (circles).

In the inset of the same figure, we analyze the small- τ dependence of the MFPT's for the right transitions $x_0 \rightarrow x_0 + nL$ with $n = 1, 2, \dots$ and reflecting barriers at $-\infty$. By applying the heuristic argument invoked to derive Eq. (4), we obtain the working approximate estimate,

$$\langle T_{R,L}^{(u)}(\tau) \rangle / \tau \simeq \exp(\Delta V / 2D_0 + nL / \sqrt{D_0 \tau}), \quad (6)$$

which holds for n -cell transitions to the right/left at vanishingly small τ . Note that here, contrary to Eq. (6), we make use of the free diffusion constant, D_0 .

Concluding remarks. The SR ratcheting mechanism introduced above can be readily generalized to more realistic cases when resetting takes a finite time¹, τ_0 , called here latency time. The relevant net ratchet speed turns out to be a function of both τ and τ_0 , $\langle v(\tau, \tau_0) \rangle$, which can

be related with the zero-latency speed, $\langle v(\tau, 0) \rangle$, through a simple time rescaling, namely

$$\langle v(\tau, \tau_0) \rangle = \langle v(\tau, 0) \rangle / (1 + \tau_0 / \tau), \quad (7)$$

as illustrated in Fig. 4(a).

This instance of SR ratchet lends itself to a simple laboratory demonstration. We start again from the LE (1) with the potential of Eq. (2) but, instead of implementing the SR protocol with latency time τ_0 , we now assume a dichotomic noise strength, $D_0(t)$, with $D_0 = 0$ for fixed time intervals, τ_0 , and $D_0(t) = D_0$ for random time intervals exponentially distributed with average τ . The resulting LE describes a rectifier, which could be classified as a special case of flashing ratchet¹⁴. In one regard the two rectification mechanisms are apparently similar: in both cases the particle rests at the bottom of a potential well for the time interval, τ_0 , before resuming Brownian diffusion, because either reset that way (SR ratchet) or given enough time to relax there (flashing ratchet with $\omega_0^2 \tau_0 \gg 1$). As shown in the inset of Fig. 4, for the same choice of the tunable parameters, D_0, τ and τ_0 , the rectification power of the two ratchets is almost identical. Therefore, one can utilize a ratchet with dichotomic noise strength to experimentally demonstrate the rectification properties of the proposed SR ratchet. However, an important difference between these two ratchets is also noteworthy. The flashing ratchet is fueled by an external source capable of “heating and cooling” the particle or its substrate^{17,23}. SR ratcheting with finite latency time, instead, can be controlled by the particle itself, by autonomously regulating its own internal motility mechanism for maximum efficiency.

In summary, we have proposed a new protocol of stochastic resetting, whereby a particle diffusing on a one-dimensional substrate, gets reset not at a fixed point,

but rather at one of the degenerate minima of the substrate. We investigated, both numerically and analytically, the diffusion properties of the reset particle and showed that for spatially asymmetric substrates the particle gets rectified with direction determined by the substrate profile, and optimal speed depending on the resetting time. We argue that, thanks to such a mechanism, a motile system (biological and synthetic, alike) can exploit the substrate asymmetry to autonomously direct its motion, for instance, by randomly switching on and off its propulsion engine at an appropriate rate.

Acknowledgements

Y.L. is supported by the NSF China under grants No. 11875201 and No. 11935010. P.K.G. is supported by

SERB Core Research Grant No. CRG/2021/007394.

Data Availability

The data that support the findings of this study are available within the article.

Conflict of interest

The authors have no conflicts to disclose.

-
- ¹ M. R. Evans, S. N. Majumdar, and G. Schehr, *Stochastic resetting and applications*, J. Phys. A: Math. Theor. **53**, 193001 (2020).
- ² L. Kusmierz, S. N. Majumdar, S. Sabhapandit, and G. Schehr, *First order transition for the optimal search time of Lévy flights with resetting*, Phys. Rev. Lett. **113**, 220602 (2014).
- ³ A. Montanari and R. Zecchina, *Optimizing searches via rare events*, Phys. Rev. Lett. **88**, 178701 (2002).
- ⁴ S. Reuveni, M. Urbakh, and J. Klafter, *Role of substrate unbinding in Michaelis–Menten enzymatic reactions* Proc. Natl. Acad. Sci. USA **111**, 4391 (2014).
- ⁵ S. Reuveni, *Optimal stochastic restart renders fluctuations in first passage times universal*, Phys. Rev. Lett. **116**, 170601 (2016).
- ⁶ S. Redner, *A Guide to First-Passage Processes* (Cambridge University Press, UK, 2001).
- ⁷ C. W. Gardiner, *Handbook of Stochastic Methods* (Springer, Berlin, 1985).
- ⁸ M. R. Evans and S. N. Majumdar, *Diffusion with stochastic resetting*, Phys. Rev. Lett. **106**, 160601 (2011).
- ⁹ A. Pal and S. Reuveni, *First passage under restart*, Phys. Rev. Lett. **118**, 030603 (2017).
- ¹⁰ A. Pal and V. V. Prasad, *First passage under stochastic resetting in an interval*, Phys. Rev. E **99**, 032123 (2019).
- ¹¹ S. Ray, D. Mondal, and S. Reuveni, *Péclet number governs transition to acceleratory restart in drift-diffusion*, J. Phys A: Math. and Theor. **52** 255002 (2019).
- ¹² J. Wang, *Nanomachines: Fundamentals and Applications* (Wiley-VCH, Weinheim, 2013).
- ¹³ P. Hänggi and F. Marchesoni, Rev. Mod. Phys. **81**, 387 (2009).
- ¹⁴ P. Reimann, *Brownian motors: Noisy transport far from equilibrium*, Phys. Rep. **361**, 57 (2002).
- ¹⁵ P. E. Kloeden and E. Platen, *Numerical Solution of Stochastic Differential Equations* (Springer, Berlin, 1992).
- ¹⁶ D. R. Cox, *Renewal Theory* (Methuen, London, 1970).
- ¹⁷ L. P. Faucheux, L. S. Bourdieu, P. D. Kaplan, and A. J. Libchaber, *Optical thermal ratchets*, Phys. Rev. Lett. **74**, 1504 (1995).
- ¹⁸ F. D. Ribetto, S. E. Deghi, H. L. Calvo, and R. A. Bustos-Marín, *A dynamical model for Brownian molecular motors driven by inelastic electron tunneling*, J. Chem. Phys. **157**, 164102 (2022).
- ¹⁹ J. Valdiviezo, P. Zhang, D. N. Beratan, *Electron ratcheting in self-assembled soft matter*, J. Chem. Phys. **155**, 055102 (2021).
- ²⁰ B. Besga, A. Bovon, A. Petrosyan, S. N. Majumdar, and S. Ciliberto, *Optimal mean first-passage time for a Brownian searcher subjected to resetting: experimental and theoretical results*. Phys. Rev. Res., **2**, 032029 (2020).
- ²¹ B. Besga, F. Faisant, A. Petrosyan, S. Ciliberto, and S. N. Majumdar, *Dynamical phase transition in the first-passage probability of a Brownian motion* Phys. Rev. E, **104**, L012102 (2021).
- ²² G. Tucci, A. Gambassi, S. N. Majumdar, and G. Schehr, *First-passage time of run-and-tumble particles with noninstantaneous resetting*, Phys. Rev. E, **106**, 044127 (2022).
- ²³ H. R. Jiang, N. Yoshinaga, and M. Sano, *Active motion of a Janus particle by self-thermophoresis in a defocused laser beam*, Phys. Rev. Lett. **105**, 268302 (2010).